

Failure Analysis of Lead-acid Batteries at Extreme Operating Temperatures

Umesh Prasad¹, Jyoti Prakash², Venkat Kamavaram³, Ganesh Arumugam³, and Arunachala Nadar Mada Kannan²

¹Affiliation not available

²Arizona State University - Polytechnic Campus

³Oceanit Laboratories Inc

February 14, 2023

Abstract

Lead-acid battery system is designed to perform optimally at ambient temperature (25 °C) in terms of capacity and cyclability. However, varying climate zones enforce harsher conditions on the automotive lead acid batteries. Hence, they age faster and exhibit low performance when operated at either extremity of the optimum ambient conditions. In this work, a systematic study was conducted to analyze the effect of varying temperatures (-10, 0, 25 and 40 °C) on the sealed lead acid. Energysys® Cyclon (2V, 5Ah) cells were cycled at C/10 rate using battery testing system. The environmental aging results in shorter cycle life due to the degradation of electrode, and grid materials at higher temperature (25 and 40 °C), while at lower temperature (-10 and 0 °C) negligible degradation was observed due to slower kinetics and reduced available capacity. Electrochemical impedance spectroscopy, X-ray diffraction and Energy-dispersive X-ray spectroscopy analysis were used to evaluate the degradation mechanism, chemical and morphological changes.

Failure Analysis of Lead-acid Batteries at Extreme Operating Temperatures

U. Prasad¹, J. Prakash¹, A. M. Kannan¹*Corresponding author amk@asu.edu*, V. Kamavaram² and G. K. Arumugam²

¹Arizona State University, 7171 E Sonoran Arroyo Mall, Mesa, AZ 85212, USA

²Oceanit Laboratories, 828 Fort Street Mall, Ste 600, Honolulu, HI 96813, USA

Abstract

Lead-acid battery system is designed to perform optimally at ambient temperature (25 °C) in terms of capacity and cyclability. However, varying climate zones enforce harsher conditions on the automotive lead acid batteries. Hence, they age faster and exhibit low performance when operated at either extremity of the optimum ambient conditions. In this work, a systematic study was conducted to analyze the effect of varying temperatures (-10, 0, 25 and 40 °C) on the sealed lead acid. Energysys® Cyclon (2V, 5Ah) cells were cycled at C/10 rate using battery testing system. The environmental aging results in shorter cycle life due to the degradation of electrode, and grid materials at higher temperature (25 and 40 °C), while at lower temperature (-10 and 0 °C) negligible degradation was observed due to slower kinetics and reduced available capacity. Electrochemical impedance spectroscopy, X-ray diffraction and Energy-dispersive X-ray spectroscopy analysis were used to evaluate the degradation mechanism, chemical and morphological changes.

Introduction

The ever-growing energy demand with the increasing population and rise in the economy has led to a rapid increase in the total energy demand globally.^{1,2} More than 80 % of the energy supplies come from carbon-rich non-renewable energy sources in the current situation.³ Battery technologies are being established rapidly due to its increasing demand in portable devices, stationary frameworks, and electric vehicles.^{4,5} Among present various battery technologies, Lead-Acid (PbA), Nickel-Metal Hydride (NiMH), Nickel-Cadmium (NiCd) and Lithium-ion (Li-ion) are the major chemistries towards different applications due to their specific characteristics related to energy density, power density, durability, and economic feasibility.⁶⁻⁸ Even though the growing popularity of Li-ion and NiMH batteries, the demand for PbA batteries grows proportionately due to their ease in availability, manufacturing, maintenance, reliability, recycling and cost.⁹ Lead acid battery demand is higher in large-scale applications such as renewable energy storage system, e.g., wind and solar technologies despite having lower energy density (< 50 Wh/kg). Lead acid battery market share is the largest for stationary energy storage system due to the development of innovative grid with Ca and Ti additives and electrodes with functioning carbon, Ga_2O_3 and Bi_2O_3 additives.^{10,11} In the current scenario, leak-proof and maintenance-free Sealed Lead Acid batteries (SLAs) are used in multiple applications such as motorcycles, ATVs, home alarm systems, toys, backup systems, workout equipment and generators.¹²⁻¹⁴

Temperature plays a key role in the battery operation as it affects the cycle life, performance, and available capacity. The PbA battery system are designed to perform optimally at ambient temperature (25°C) for performance, capacity and cyclability. However, they degrade faster when operated at higher than ambient conditions leading to shorter cycle life due to the degradation of electrode and grid materials.⁶ The oxidation and reduction rates increase significantly at both Pb anode and PbO_2 cathode, leading to higher discharge capacity at elevated temperatures.^{7,12} Besides having a deleterious impact on the cycle life at elevated temperatures, several other impacts include self-discharge reactions, loss of electrolyte, active material shedding, grid corrosion, and loss of mechanical strength of the positive electrode (PbO_2).¹⁵⁻¹⁷ Shedding or loss of positive active mass particles into the electrolyte could also increase corrosion and macro defects on the lugs of the negative electrode.^{16,17} While operating at lower temperature, low electrolyte conductivity and active material results in reduced available capacity.⁶ To reduce the corrosion or degradation rate of the PbA battery, limiting the internal temperature to $< 60^\circ\text{C}$ could minimize the electrolyte vaporization.¹⁸ The cell internal pressure should be in acceptable range for long term optimum performances. However, it was reported that charging efficiency and cyclability were improved under high internal pressure with the favorable crystal structure of the electrodes.¹⁶ Performance evaluation of the batteries at elevated temperatures and near-freezing temperature is critical for using these batteries for outdoor energy storage applications in hot and cold conditions.⁶

The adverse effect of temperature also includes reduced discharge capacity, increased internal resistance and self-discharge with increased duration at extreme temperatures. Typical PbA batteries undergo many charge/discharge cycles during their life time.¹⁰ Hence it is necessary to understand the complete cycling behavior of PbA battery in various operating conditions, including incomplete charging, slow discharging, extreme conditions such as temperature fluctuations, and vibrations that cause degradation of internal components leading to failure of the battery.

In this work, a systematic study was conducted to analyze the 2V/5Ah Energysys® Cyclon sealed lead-acid (SLA) cells cycled at -10 , 0 , 25 and 40°C , to minimize the experimentation duration as these conditions are practical for vehicles used or stored in frozen tundra and arid desert climates. To evaluate these condition, electrochemical impedance spectroscopy (EIS) was carried out to evaluate internal resistance (ohmic and charge transfer) to explain the degradation mechanism of the battery. Further, electrode materials were extracted post cycling analysis for morphology characterization using X-ray diffraction (XRD), and Energy-dispersive X-ray spectroscopy analysis (EDX). SLA batteries were observed to degrade faster at higher temperatures (25 and 40°C). However, the degradation is minimal at lower temperatures (0 and -10°C) due to less active material and slower kinetics. The impedance values, x-axis intercept of Nyquist plot was observed to increase with cycling at all the temperatures.

Experiments Setup

Sealed lead acid cells 2 V, 5 Ah (Cyclon Enersys®) were tested in this study at -10, 0, 25 and 40 °C (Figure 1a). Studies on these temperature margins are sufficient to provide better understanding of SLA cell performance. The thermal chamber (ESPEC, BTU-433) was used for testing cells in a controlled environment (Figure 1b). A programmable battery tester (Arbin Instruments, BT-1) was used for charge/discharge cycling studies. The charge and discharge cut-off potential were kept at 2.45 and 1.85 V, with a constant charging and discharging rate of C/10 (0.5 A) and a 5 min rest period between charging and discharging cycles. The discharge rate was taken to study the slow charge discharge phenomena. Discharge capacities were calculated for each cycle from the charge and discharge profiles. EIS spectra were recorded after 20/25 charge-discharge cycles in fully charged state at room temperature using a potentiostat/galvanostat (PARSTAT 2273, Princeton Applied Research) with a frequency range of 10 Hz to 1 kHz.



Figure 1: (a) Cyclon cell 2V and 5 Ah (b) temperature controlled environmental chamber.

Post cycling analysis, electrode materials were extracted in charged and discharged states for chemical and morphological characterization (Figure 2). The extracted material was thoroughly ground, rinsed with water profusely to remove remnant acid, and dried overnight at 80 °C. Phase and crystal structure of pristine and degraded electrodes were examined using XRD (PANalytical X'Pert PRO MRD; Cu K α radiation; 0.006 degrees/sec). Phases of the materials were validated after rinsing and drying process during material extraction process. EDX spectral mapping analysis (25 kV) was performed for estimating the chemical composition of electrodes post degradation.

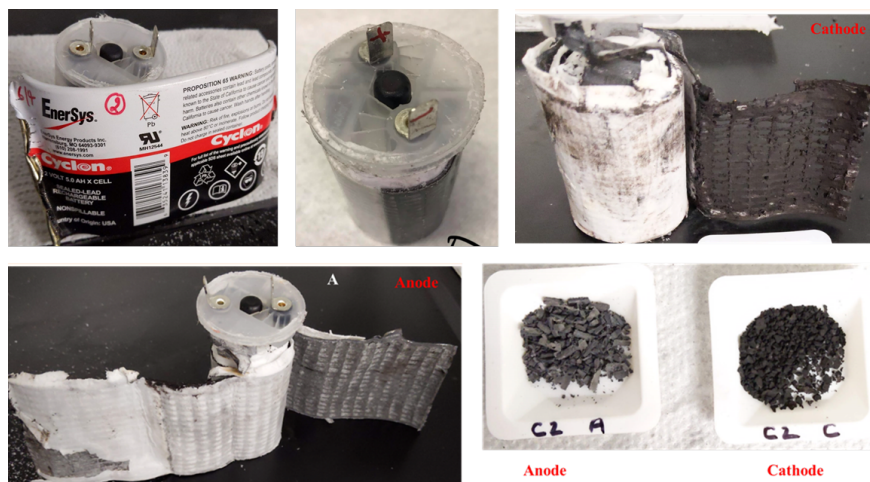


Figure 2: Cell disassembling process after cycling studies to extract active electrode materials for XRD characterization.

Result and Discussion:

The charge-discharge profiles at different operating temperatures, electrochemical impedance spectra studies, chemical and morphological analysis are discussed in the following sections.

Charge-Discharge Cycling Studies:

The discharge profiles of the cycled cells at -10, 0, 25 and 40 °C are shown in Figure 3a-d. It was observed that during the initial cycles the total discharge duration at 40 and 25 °C is about 2X as compared to that at 0 and -10 °C, which is due to slower kinetics and lower electrolyte conductivity. Moreover, the discharge duration are 2, 2.5, 3.8 and 1.5 h after 120 cycles for 40, 25, 0 and -10 °C, respectively. This suggests that ageing of PbA battery is faster at elevated temperature (40 and 25 °C) than at sub-ambient temperatures (0 and -10 °C). For cell discharged at 0 °C, the total discharging duration remains unchanged throughout the cycling studies. Whereas for cell discharged at -10 °C the discharge duration decreases from 3.5 to 1.5h, which is relatively faster ageing despite low active materials utilization due to reduced initial available capacity.

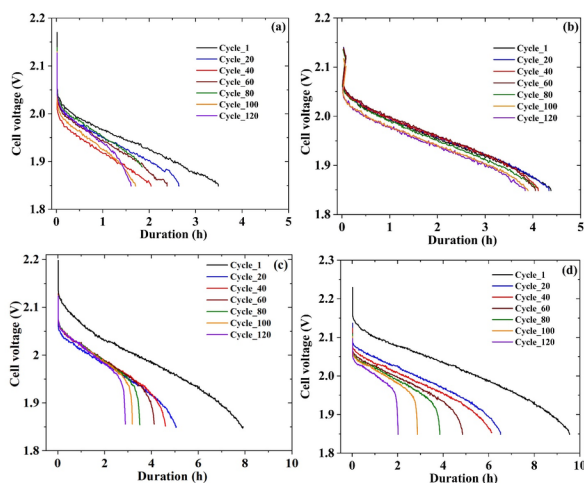


Figure 3: Discharge curves at C/10 rate for (a) -10 °C, (b) 0 °C, (c) 25 °C and (d) 40 °C

Figure 4a-d illustrates the charging pattern of the cells at -10, 0, 25 and 40 °C. Similar to discharging profiles, during the initial cycles it was observed that total charging duration is higher for cells discharged at 40 and 25 °C, as compared to that at 0 °C and -10 °C. The charge durations are 2, 2.5, 4 and 1.5 h after 120 cycles for 40, 25, 0 and -10 °C, respectively. Similar charging and discharging patterns corroborate the observed capacity degradation process.

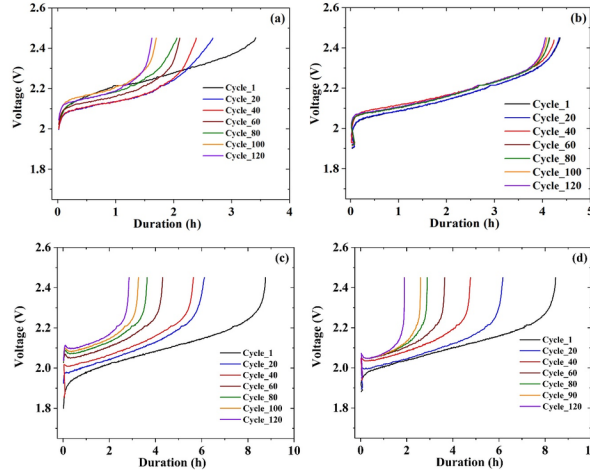


Figure 4: Charge curves at C/10 rate for (a) -10 °C, (b) 0 °C, (c) 25 °C and (d) 40 °C

Discharge capacity of the cells calculated from the discharge profiles is illustrated in Figure 5a. It was observed that discharge capacity is close to the theoretical capacity (5Ah) for 25 °C and 40 °C, while the initial discharge capacity at -10 °C is higher than the result at 0 °C, the discharge capacity drop is much significant in -10 °C because lower temperature increases the internal resistance and reduces the capacity.¹⁹ Steep slope confirms that degradation is higher at 40 °C due to enhanced ageing of the electrodes from faster reaction kinetics at elevated temperature. The capacity degradation after 130 cycles are 92, 74, 69 and 17% for 40, -10, 25 and 0 °C, respectively. Moreover, the cell degradation is insignificant at 0 °C even though the total discharge capacity is low. The state of health (SOH) is a measurement that reflects the general condition and ability to deliver the specified performance compared to that of a fresh battery. SOH takes into consideration factors such as charge acceptance, internal resistance, voltage, and self-discharge.^{4,20,21} It is a measure of the battery's long-term capability and available lifetime energy throughput. Health of the battery tends to deteriorate gradually due to irreversible physical and chemical changes, hence SOH is estimated by multiple methods including impedance, conductance and discharge capacity (current/actual).^{4,20} SOH was calculated using instant discharge capacity and initial capacity (after 1st cycle) as illustrated in Figure 5b. SOH was observed to be highest for 0 °C ranging from 95% (1st cycle) to 89% (130th cycle). However, the SOH decreased sharply for cells discharged at -10 °C (78% to 46%), 25 °C (67 to 28%), and 40 °C (73 to 10%). Significant SOH loss was observed for 40 °C confirming major degradation.

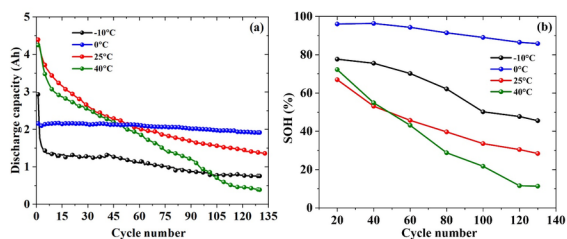


Figure 5: (a) Discharge capacities and (b) SOH of the cells at -10, 0, 25 and 40 °C .

Electrochemical Impedance Spectroscopy Studies:

Electrochemical impedance spectroscopy (EIS) was measured after every 20/25 charge-discharge cycles at room temperature and in fully charged state. EIS is essential for evaluating the power loss due to cycling and analyzing the failure mechanism. The Nyquist plots of the cells discharged at different temperatures are illustrated in Figure 6 a-d. All the cells initial showed similar impedance values (0.05 – 0.06 Ω) prior to cycling. However, after 130 cycles the impedance values are significantly higher: 0.41, 0.20, 0.13, and 0.38 Ω at -10, 0, 25, and 40 °C, respectively. The increase in impedance is consistent with capacity degradation after 130 cycles as shown in Figure 5a.

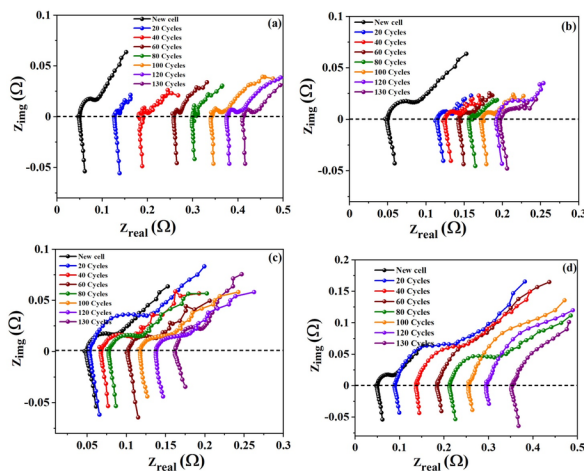


Figure 6: Electrochemical impedance spectroscopy at (a) -10, (b) 0, (c) 25 and (d) 40 °C .

According to the standard equivalent circuit model, the measured impedance data were analyzed by using a complex non-linear least squares (CNLS) fitting method (Figure 7). EIS studies the system response to the application of a periodic small amplitude AC signal.^{5,10} Analysis of the system response contains information about the interface, its structure and reactions taking place at the interfaces e.g., electrolyte-electrodes.²⁰

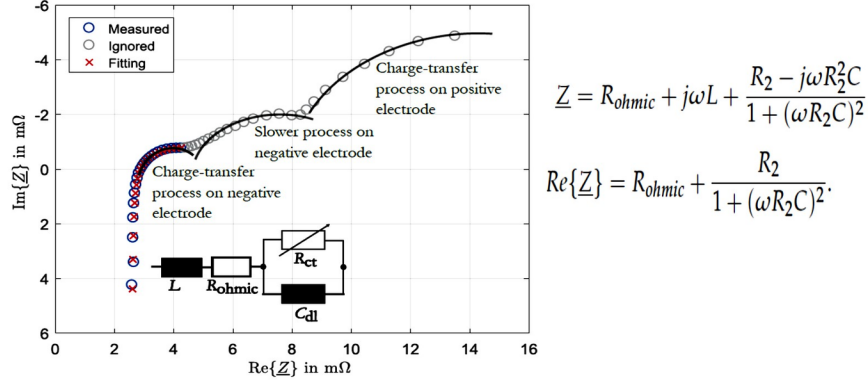


Figure 7: Equivalent circuit model representing lead-acid battery. ²⁰

The impedance value, x-intercept from the Nyquist plot (Figure 6 a-d), is observed to increase gradually with cycling for all the temperatures (Figure 8a). However, the increase is higher at low temperatures (-10 & 0 °C) than at higher temperatures (25 & 40 °C) even though the total active material availability and utilization is significantly reduced at the lower temperatures. The lower real impedance at higher temperatures (25 and 40 °C) essentially means that battery activity is improved despite higher degradation.

The ohmic and charge transfer resistance were calculated by fitting the EIS data to equivalent circuit model using *ZSimpWin* software. The ohmic resistance and charge transfer resistances exhibited similar behavior as impedance values (Figure 8b and 8c). However, it is reported that charge transfer resistance is critical in representing the degradation mechanism as it reflects the reaction mechanism at electrodes.^{10,20,22} The voltage at 50% discharge cycle ($V_{dis,50\%}$) was analyzed to further evaluate the capacity degradation with cycling (Figure 8d). These values increase with cycles at all temperatures, however, more rapidly at 25 and 40 °C than at 0 and -10 °C. Higher battery degradation correlates to higher slope of the $V_{dis,50\%}$ vs cycle profiles, which essentially shows that the cell discharge capacity and SOH are decreasing with cycling.

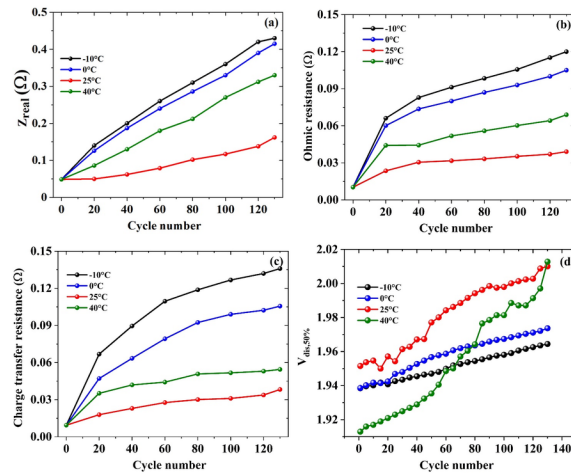


Figure 8: (a) Impedance, (b) ohmic resistance, (c) charge transfer resistance and (d) $V_{dis,50\%}$ with cycle numbers for -10, 0, 25 and 40 °C.

Chemical and Morphological Analysis:

Two cells were cycled at each temperature for data reliability and XRD analysis. The anode and cathode materials obtained from the fresh and cycled cells in charged and discharged states were analyzed using XRD (Figure 9).

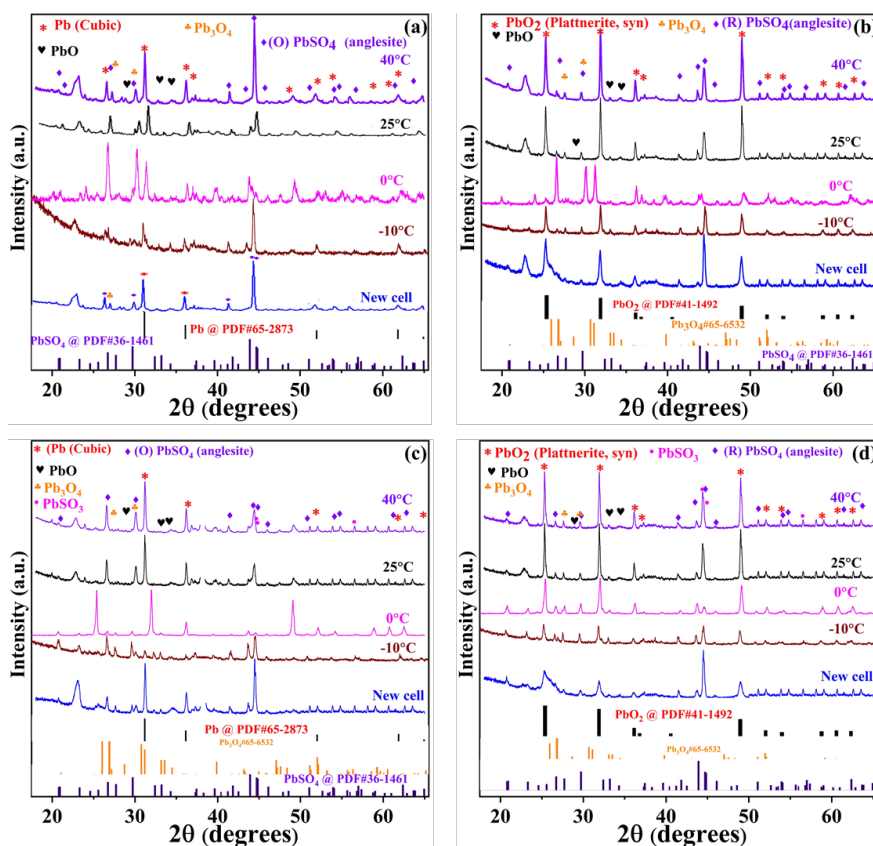


Figure 9: (a) Anode, and (b) cathode in fully charged condition after 130 cycles, (c) anode and (d) cathode in discharged condition after 130 cycles for cells cycled at -10, 0, 25 and 40 °C.

The XRD pattern of anode after 130 cycles in charged condition contained Pb (cubic) and PbSO_4 (anglesite) peaks, like that for the fresh cells (Figure 9a). Along with Pb and PbSO_4 , there were PbO, Pb_3O_4 peaks for the cycled cell at different temperatures (Figures 9 a-d). Pb peaks intensity was higher and sharper in the new cell than the cycled cells, which confirmed that the PbSO_4 was completely converting into Pb through reduction reaction. However, there was a permanent deposition of PbSO_4 in the cycled cells after 130 cycles due to surface hardening. The intensity of PbSO_4 peaks was more intense at 40 °C compared to 25 °C and new cell, which could be attributed to poor reversibility with a higher amount of PbSO_4 at the anode in the charge condition (Figure 9a).

The cathode in charged condition contained PbO_2 and PbSO_4 peaks, like that of the fresh cells (Figure 9b). The cell after 130 cycles also showed Pb, PbO, and Pb_3O_4 peaks. The PbO_2 peaks intensity was higher and sharper in the fresh cell than the cycled cell after 130 cycles. PbSO_4 detected due to permanent deposits (surface hardening) through charge/discharge cycling, leading to capacity loss. The PbSO_4 peaks was more intense at 40 °C compared to those cycled at 25 °C and fresh cell due to accelerated kinetics at higher temperature leading to irreversibility. However, there was not much difference observed in the cells at 0 °C in charged (Figure 9a) than cell in discharged state (Figure 9c). This could be because at 0 °C only half of the cell capacity was used, discharge capacity is 4.1 Ah at 25 °C and 2.15 Ah at 0 °C due to the change in kinetics at 0 °C temperature. Similarly, at -10 °C the cathode for the cell after 130 cycles in charged and discharged

condition contained PbO_2 , Pb_3O_4 and PbSO_4 peaks (Figure 9b & d). However, at 0 °C, the anode both in charged and discharged conditions contained Pb (cubic), PbO and PbSO_4 (anglesite) peaks (Figure 9a & c).

The anode in discharged condition for the cell after 130 cycles contained the Pb (cubic) and PbSO_4 (anglesite) peaks, like that of the fresh cells (Figure 9c). Along with Pb and PbSO_4 , there were $\text{Pb}_3\text{O}_2\text{SO}_4$, PbSO_3 , PbO, and Pb_3O_4 peaks in the cell after 130 cycles. The PbO, PbSO_4 , and Pb_3O_4 peaks were identified in Figures 9c & 9d. The $\text{Pb}_3\text{O}_2\text{SO}_4$ peaks were not detected in XRD, but they do exist in charging condition. The PbSO_4 peaks intensity was higher and sharper in the fresh cell compared to the cell after 130 cycles, mostly agglomerated and surface hardened active materials, which confirmed that the Pb was completely converting into PbSO_4 through an oxidation reaction in the fresh cell.^{6,17,18,23} Some of the PbSO_4 peaks such as 26.6°, 29.8° and 36° are relatively higher in the cycled cell compared to the fresh cells. However, the main peak intensity at 44.4° is more intense in the fresh cell than cycled cells. This discrepancy observed could be attributed to the compositional difference on the electrode surface and in the bulk. The Pb peaks were more intense at 40 °C compared to that at 25 °C and fresh cell, this is probably due to higher deposition of Pb at anode in the charged condition.^{6,23}

The cathode in discharged condition contained PbO_2 and PbSO_4 peaks for the cycled cells, like that with the fresh cells (Figure 9d). Moreover, the cell after 130 cycles also showed $\text{Pb}_3\text{O}_2\text{SO}_4$, PbSO_3 , Pb, PbO, and Pb_3O_4 peaks. The PbSO_4 peaks intensity were higher and sharper in the new cell compared to the cell after 130 cycles. The PbO_2 detected could be due to the inability of the bulk active material not being able to get reduced during discharge at elevated temperature, leading to less utilization of active materials and faster capacity fading/degradation in the cycled cell. Obviously, the PbO_2 peaks was more intense at 40 than compared to 25 °C and the fresh cell due to larger deposition of PbO_2 at the cathode in the charged condition.^{13,14} There was not much difference observed in the Pb peak intensity in charge condition for cathode (Figure 9b) and cell at discharge condition (Figure 9d) at 0 °C. Similar to anode, this could be because at 0°C only half of the cell capacity was used due to the slower kinetics at this temperature. In summary, the XRD analysis concludes that the major/minor phases in charged and discharged state for electrodes are as illustrated in Table 1.

Table 1: Summary of phases present in the electrode from XRD analysis.

Electrodes	Status	Phase
Anode	Charged	Pb (cubic) (Major) (O) PbSO_4 : anglesite (Minor)
Anode	Discharged	Pb (cubic) (Minor) (O) PbSO_4 : anglesite (Major)
Cathode	Charged	PbO_2 : plattnerite (Major) (R) PbSO_4 : anglesite (Minor)
Cathode	Discharged	PbO_2 : plattnerite (Minor) (R) PbSO_4 : anglesite (Major)

Note: O – oxidation and R – reduction

The energy-dispersive X-ray spectroscopy (EDS) was conducted on anode and cathode active materials for examining sulfur content which is represented as the Pb/S ratio. The Pb/S is the ratio of composition obtained from the Pb, PbO_2 and PbSO_4 peaks in EDS spectrum (Table 2). Higher values of Pb/S means lower SO_4^{2-} content and vice versa. The Pb/S ratio indicative of the relative amount of sulfate (SO_4^{2-}) getting deposited on anode and cathode after cycling. Pb/S ratio of the fresh cell is significantly different due to complete reversibility of PbSO_4 to Pb as compared to that observed in cycled cells. As indicated from Pb/S ratio it can be seen that SO_4^{2-} deposition and hardening were higher in anode and cathode in discharged state which eventually led to reduction in the amount of active materials with cycling (130 cycles).^{21,22,24} It can be seen that SO_4^{2-} content increases with decreasing temperature from 40 to 0 °C due to slower

kinetics and lower PbSO₄ reversibility to Pb. However, it is lowest at -10 °C as compared to cycled and fresh cells essentially due to reduced active material (~50%) availability as seen from the charge-discharge characteristics (Figures 3-5).^{6,18,25}

Table 2: EDS chemical analysis comparison of the electrodes from cycled cells (130 cycles) at various temperatures and fresh cells.

Electrodes from cycle cells	Electrodes from cycle cells	Pb/S ratio Fresh	Pb/S ratio 40 °C	Pb/S ratio 25 °C	Pb/S ratio 0 °C
Anode	Charged	48.5 ± 2.43	24.2 ± 1.24	26.3 ± 1.31	21.3 ± 1.07
	Discharged	23.3 ± 0.012	17.8 ± 0.9	15.4 ± 0.77	15.3 ± 0.77
Cathode	Charged	55.3 ± 2.81	24.0 ± 1.25	27.0 ± 1.36	22.5 ± 1.3
	Discharged	21.6 ± 1.09	20.1 ± 1.1	16.1 ± 0.83	13.1 ± 0.7

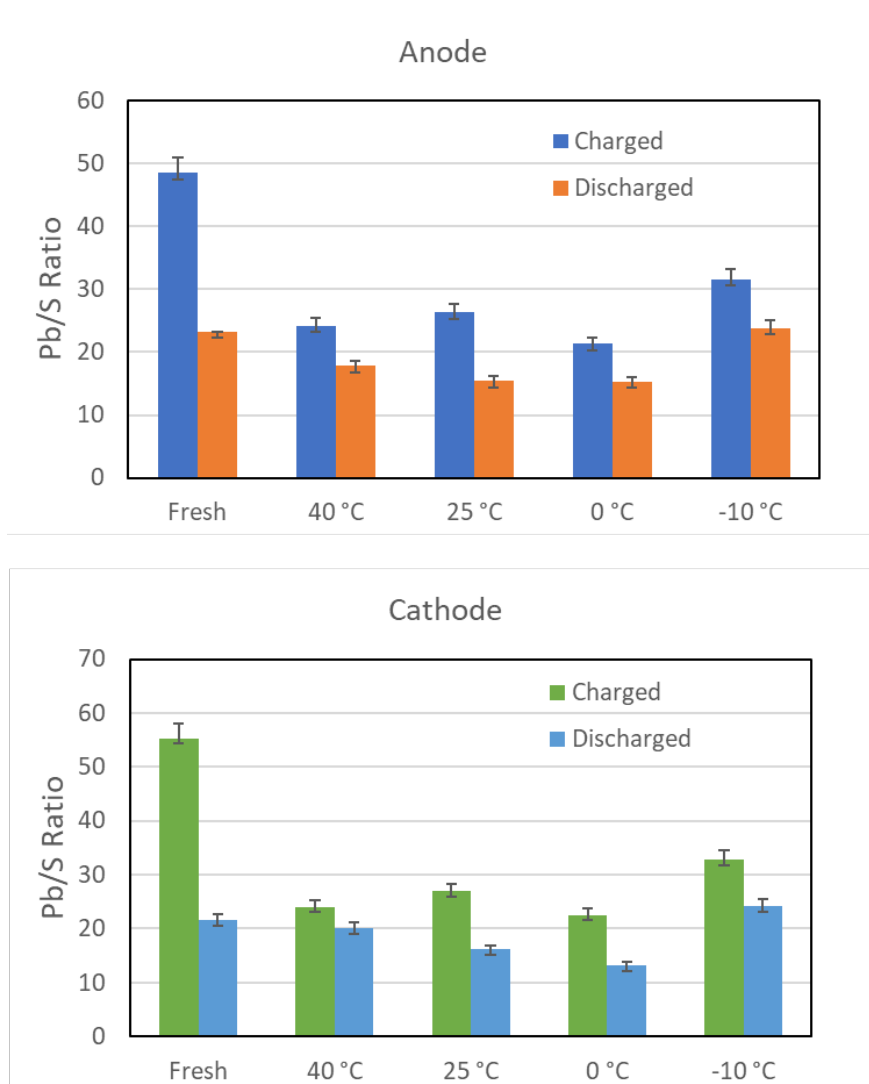


Figure 10: EDS chemical analysis comparison of the electrodes from cycled cells (130 cycles) at various

temperatures and fresh cells. (Table 2 data is represented as histograms.)

Conclusion:

The sealed lead acid (SLA) cells were cycled at -10, 0, 25 and 40 °C to evaluate the performance and degradation mechanism. Discharge profiles demonstrated that the ageing is faster at elevated temperature (40 °C) than at lower temperature (-10, 0, & 25 °C). However, capacity degradation is minimal at 0 and -10 °C due to reduced active material availability. Moreover, EIS analysis revealed that impedance change was significantly higher at 25 and 40 °C as compared to that at 0 and -10 °C. The charge transfer resistance is relatively more governing factor than ohmic resistance for indicating the degradation of the cell. XRD analysis revealed that a permanent deposition of SO₄ due to surface hardening (usually termed as sulfate hardening) in the cells after cycling at all the temperatures. However, sulfate hardening is significantly higher at 25 and 40 °C as compared to that at 0 and -10 °C as confirmed from Pb/S ratio determined from EDS analysis. The study demonstrates that temperature of operation plays a crucial role in state of health prediction of sealed lead -acid batteries.

Acknowledgements

The authors acknowledge financial support from US Army Research Office, Oceanit and Arizona State University. V. Kamavaram and G. K. Arumugam acknowledge financial support from US Army Research Office (W911NF-18-C-0083).

References:

- (1) Prasad, U.; Prakash, J.; K. Gupta, S.; Zuniga, J.; Mao, Y.; Azeredo, B.; Nadar Mada Kannan, A. Enhanced Photoelectrochemical Water Splitting with Er- and W-Codoped Bismuth Vanadate with WO₃ Heterojunction-Based Two-Dimensional Photoelectrode. *ACS Appl. Mater. & Interfaces* **2019** , *11* , 19029–19039.
- (2) Prasad, U.; Young, J. L.; Johnson, J. C.; McGott, D. L.; Gu, H.; Garfunkel, E.; Kannan, A. M. Enhancing Interfacial Charge Transfer in a WO₃ /BiVO₄ Photoanode Heterojunction through Gallium and Tungsten Co-Doping and a Sulfur Modified Bi₂O₃ Interfacial Layer . *J. Mater. Chem. A* **2021** , *9* , 16137–16149.
- (3) Prasad, U. BiVO₄-Based Photoanodes for Photoelectrochemical Water Splitting. *ACS Symp. Ser.* **2020** , *1364* , 137–167.
- (4) Vignarooban, K.; Chu, X.; Chimatapu, K.; Ganeshram, P.; Pollat, S.; Johnson, N. G.; Razdan, A.; Pelley, D. S.; Kannan, A. M. State of Health Determination of Sealed Lead Acid Batteries under Various Operating Conditions. *Sustain. Energy Technol. Assessments* **2016** ,*18* , 134–139.
- (5) Vaidya, R.; Selvan, V.; Badami, P.; Knoop, K.; Kannan, A. M. Plug-In Hybrid Vehicle and Second-Life Applications of Lithium-Ion Batteries at Elevated Temperature. *Batter. Supercaps* **2018** , *1* , 75–82.
- (6) May, G. J.; Davidson, A.; Monahov, B. Lead Batteries for Utility Energy Storage: A Review. *J. Energy Storage* **2018** ,*15* , 145–157.
- (7) Sun, Z.; Cao, H.; Zhang, X.; Lin, X.; Zheng, W.; Cao, G.; Sun, Y.; Zhang, Y. Spent Lead-Acid Battery Recycling in China – A Review and Sustainable Analyses on Mass Flow of Lead. *Waste Manag.***2017** , *64* , 190–201.
- (8) Zakiyya, H.; Distya, Y. D.; Ellen, R. A Review of Spent Lead-Acid Battery Recycling Technology in Indonesia: Comparison and Recommendation of Environment-Friendly Process. *IOP Conf. Ser. Mater. Sci. Eng.***2018** , *288* .
- (9) Saravanan, M.; Ganesan, M.; Ambalavanan, S. A Modified Lead-Acid Negative Electrode for High-Rate Partial-State-of-Charge Applications. *J. Electrochem. Soc.* **2012** , *159* , A452–A458.
- (10) Krivík, P.; Vaculík, S.; Bača, P.; Kazelle, J. Determination of State of Charge of Lead-Acid Battery by EIS. *J. Energy Storage***2019** , *21* , 581–585.

- (11) Pavlov, D. The Lead-Acid Battery Lead Dioxide Active Mass: A Gel-Crystal System with Proton and Electron Conductivity. *J. Electrochem. Soc.* **1992** , 139 , 3075–3080.
- (12) Doerffel, D.; Sharkh, S. A. A Critical Review of Using the Peukert Equation for Determining the Remaining Capacity of Lead-Acid and Lithium-Ion Batteries. *J. Power Sources* **2006** ,155 , 395–400.
- (13) Moseley, P. T.; Rand, D. A. J.; Davidson, A.; Monahov, B. Understanding the Functions of Carbon in the Negative Active-Mass of the Lead–Acid Battery: A Review of Progress. *J. Energy Storage***2018** , 19 , 272–290.
- (14) Li, M.; Yang, J.; Liang, S.; Hou, H.; Hu, J.; Liu, B.; Kumar, R. V. Review on Clean Recovery of Discarded/Spent Lead-Acid Battery and Trends of Recycled Products. *J. Power Sources* **2019** , 436 , 226853.
- (15) Zou, C.; Zhang, L.; Hu, X.; Wang, Z.; Wik, T.; Pecht, M. A Review of Fractional-Order Techniques Applied to Lithium-Ion Batteries, Lead-Acid Batteries, and Supercapacitors. *J. Power Sources***2018** , 390 , 286–296.
- (16) Zguris, G. C. A Review of Physical Properties of Separators for Valve-Regulated Lead/Acid Batteries. *J. Power Sources***1996** , 59 , 131–135.
- (17) Singh, A.; Karandikar, P. B. A Broad Review on Desulfation of Lead-Acid Battery for Electric Hybrid Vehicle. *Microsystem Technologies* . 2017, pp 2263–2273.
- (18) Dürr, M.; Cruden, A.; Gair, S.; McDonald, J. R. Dynamic Model of a Lead Acid Battery for Use in a Domestic Fuel Cell System. *J. Power Sources* **2006** , 161 , 1400–1411.
- (19) Hariprakash, B.; Mane, A. U.; Martha, S. K.; Gaffoor, S. A.; Shivashankar, S. A.; Shukla, A. K. A Low-Cost, High Energy-Density Lead/Acid Battery. *Electrochem. Solid-State Lett.* **2004** , 7 .
- (20) Kwiecien, M.; Badeda, J.; Huck, M.; Komut, K.; Duman, D.; Sauer, D. U. Determination of SoH of Lead-Acid Batteries by Electrochemical Impedance Spectroscopy. *Appl. Sci.* **2018** , 8 , 1–23.
- (21) De Marco, R.; Jones, J. Changes in Positive Lead/Acid Battery Plates during Charge/Discharge Cycling. *J. Appl. Electrochem.***2000** , 30 , 77–83.
- (22) Pavlov, D.; Petkova, G.; Dimitrov, M.; Shiomi, M.; Tsubota, M. Influence of Fast Charge on the Life Cycle of Positive Lead-Acid Battery Plates. *J. Power Sources* **2000** , 87 , 39–56.
- (23) Zhang, B.; Zhong, J.; Li, W.; Dai, Z.; Zhang, B.; Cheng, Z. Transformation of Inert PbSO₄ Deposit on the Negative Electrode of a Lead-Acid Battery into Its Active State. *J. Power Sources***2010** , 195 , 4338–4343.
- (24) Pavlov, D.; Kirchev, A.; Stoycheva, M.; Monahov, B. Influence of H₂SO₄ Concentration on the Mechanism of the Processes and on the Electrochemical Activity of the Pb/PbO₂/PbSO₄ Electrode. *J. Power Sources* **2004** , 137 , 288–308.
- (25) Pavlov, D. Suppression of Premature Capacity Loss by Methods Based on the Gel-Crystal Concept of the PbO₂ Electrode. *J. Power Sources* **1993** , 46 , 171–190.